Solution of the Young-Laplace equation for three particles

P. R. Rynhart[1] , R. McLachlan[1] , J. R. Jones[2] & R. McKibbin[3]

[1] *Institute of Fundamental Sciences*
Massey University, Palmerston North, New Zealand.

[2] *Institute of Technology & Engineering*
Massey University, Palmerston North, New Zealand.

[3] *Institute of Information & Mathematical Sciences*
Massey University at Albany, Auckland, New Zealand.

This paper presents the solution to the liquid bridge profile formed between three equally sized spherical primary particles. The particles are equally separated, with sphere centres located on the vertices of an equilateral triangle. Equations for the problem are derived and solved numerically for given constant mean curvature H_0, contact angle α, and inter-particle separation distance S. The binding force between particles is calculated and plotted as a function of liquid bridge volume for a particular example. Agreement with experiment is provided.

1   INTRODUCTION

The profile and properties of liquid bridges between rigid solid spheres is governed by the Young-Laplace equation. This equation relates the mean curvature of the bridge surface to the pressure deficiency due to the presence of the fluid (ΔP). De Bisschop and Rigole (1) used numerical integration to solve the Young-Laplace equation between two particles. Given the radii of the particles, half-filling angles and the separation distance between particles, they were able to calculate the surface area, volume, inter-particle force and Gibbs free surface energy to form a solution space where the mean curvature was a parameter. Using the Gibbs free surface energy, liquid bridge stability criteria was derived. Rynhart *et. al* (2) presented the solution as a phase portrait, in which the force is related to the liquid bridge shape.

Recently Urso *et al.* (3) analysed the Young-Laplace equation in two dimensions, using circular arcs, to estimate properties of pendular, funicular and capillary state liquid bridges. Based on this work, they relate the inter-particle force of attraction to the fluids to solids volume ratio, and to the fluid contact angle. Their work shows decreasing force with decreasing fluids to solids ratio. In this paper, we present a method of solution for capillary state liquid bridges between three particles in three dimensions. The particles are equally sized of radius a, and are equi-distant from each other. Properties of the liquid bridges that are able to be calculated include the surface area, volume and inter-particle force. The Young-Laplace equation is numerically integrated in a similar way to the work of De Biscchop and Rigole (1).

For an interface at thermodynamic equilibrium, the Young-Laplace equation must be satisfied (4),

$$H_0 = \frac{\Delta P}{\gamma}, \tag{1.55}$$

as the fluid surface is required to have constant mean curvature H_0. In equation (1.55), ΔP is the difference in fluid pressure associated with passing from external (ambient) pressure towards the centre of the liquid surface, and γ is the surface tension. The analogous configuration of two particles has cylindrical symmetry which allows a second order ordinary differential equation to be derived (1). For the three particle problem, this symmetry does not exist, and therefore another approach is required.

Allowing z to denote the height the fluid surface, the surface is parameterised using cylindrical coordinates r and θ such that $z = z(r, \theta)$ as illustrated in figure 54. The transformation between cylindrical and Cartesian coordinates (X, Y, Z) is given by

$$\mathbf{Z}(r, \theta) = (X, Y, Z) = (r, z \cos \theta, z \sin \theta), \tag{1.56}$$

where $\mathbf{Z}$ is the surface in Cartesian coordinates. Due to symmetry, it is sufficient to solve the problem for only 1/12 of the complete fluid surface. This is because the surface is mirrored about the Z axis, and because the surface can be divided into six reflected regions. The problem is $\frac{\pi}{2}$ periodic with respect to θ. As a result, the fluid profile is solved for the shaded region in figure 54. Boundary conditions for the problem are the contact angle α between the liquid and solid surfaces which occurs at the three phase contact contour, C_1. Continuity of the surface is required along contour C_2, which is referred to in this work as the symmetry contour because it bisects the liquid bridge between adjacent particles. The problem is arranged using an r axis, which is aligned from the centre point of one of the primary particles at $r = 0$ to the central point of the liquid bridge at $r = r_0$. The plan view presented in figure 54 corresponds to the case $\theta = \frac{\pi}{2}$; in this view the angle ϕ formed between the r axis and the symmetry contour is 60 deg. When $\theta = 0$, the arrangement of figure 54 is an elevation view (side-on), and the angle between the r axis and contour C_2 is 90 deg. For intermediate values of θ, the angle between the r axis and the symmetry contour C_2 varies smoothly between 60 deg and 90 deg.

Equation (1.55) is enforced by expressing the mean curvature H_0 in terms of z and the partial derivatives of z. This paper explains how to introduce an appropriate coordinate system to analyse the problem, and how to obtain a solution using a robust non-linear equation solver.

Figure 55 shows an enlarged view of the section of surface that will be solved. For a given θ, the value of r at which the three phase contact line occurs is r_s. Along C_2, the symmetry contour intersects the fluid surface at r position r_p. Using figure 55 and trigonometry, for a sphere of radius a, the relationship between the dimension r_0 and the inter-particle separation distance S is

$$r_0 = r_\mathrm{p} + (r_0 - r_\mathrm{p}) = \left(\frac{\sqrt{3}}{2} + \frac{1}{2\sqrt{3}} \right) \left(a + \frac{S}{2} \right) = \frac{2}{\sqrt{3}} \left(a + \frac{S}{2} \right). \tag{1.57}$$

2 DERIVATION OF THE EQUATIONS

In differential geometry, surfaces are able to be described by two quadratic differential forms, known as the first and second fundamental forms (5). By expressing the surface $z(r, \theta)$ in terms of these functions, it is possible to derive the following second order non-linear elliptic partial differential equation (6) for the mean curvature,

$$H = \frac{z^2 - zz_{\theta\theta} + 2z_\theta^2 + z_r^2 z^2 - zz_{\theta\theta} z_r^2 + 2zz_{r\theta} z_r z_\theta - z_{rr} z^3 - zz_{rr} z_\theta^2}{2 \left(z_\theta^2 + z^2 (1 + z_r^2) \right)^{\frac{3}{2}}} = \frac{P}{Q}, \tag{2.58}$$

where P and Q are the numerator and denominator of H. In equation (2.58), standard notation has been used for the derivatives; for example, $z_{r\theta} = \frac{\partial^2 z}{\partial \theta \partial r}$. In order for the surface $z(r, \theta)$ to have constant mean curvature H_0, thus satisfying equation (1.55), equation (2.58) must be satisfied at all points on the fluid surface.
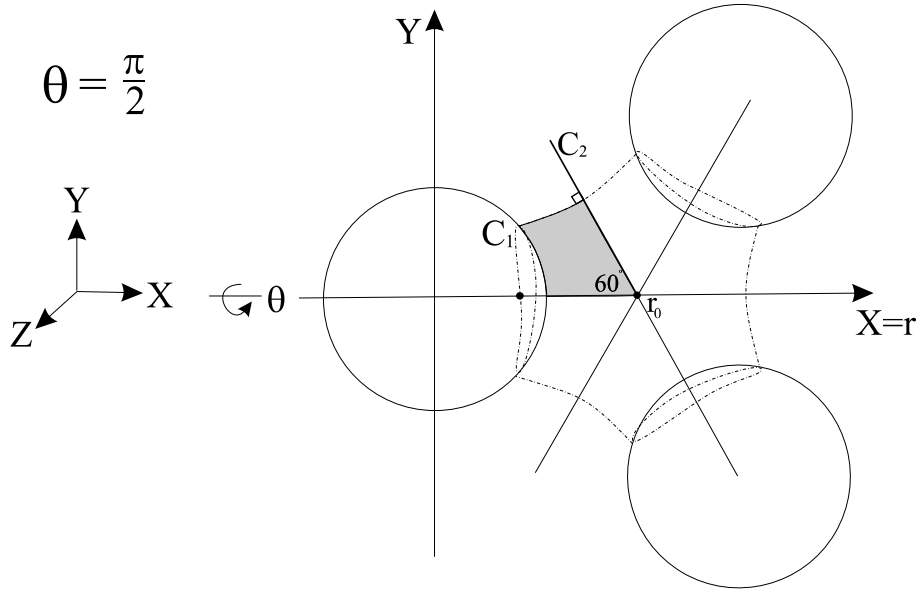
$$\theta = \frac{\pi}{2}$$

Figure 54: Cross-section of a liquid bridge between three particles for $\theta = \frac{\pi}{2}$. The dotted outline is the boundary of the fluid surface z. The contact angle α occurs along contour C_1, and the symmetry contour intersects the r along C_2. The view is a cross-section for $\theta = \frac{\pi}{2}$ where the angle between the symmetry contour and the r axis is 60 deg. When $\theta = 0$ (perpendicular to the view shown here) the angle between the symmetry contour and the r axis is 90 deg.
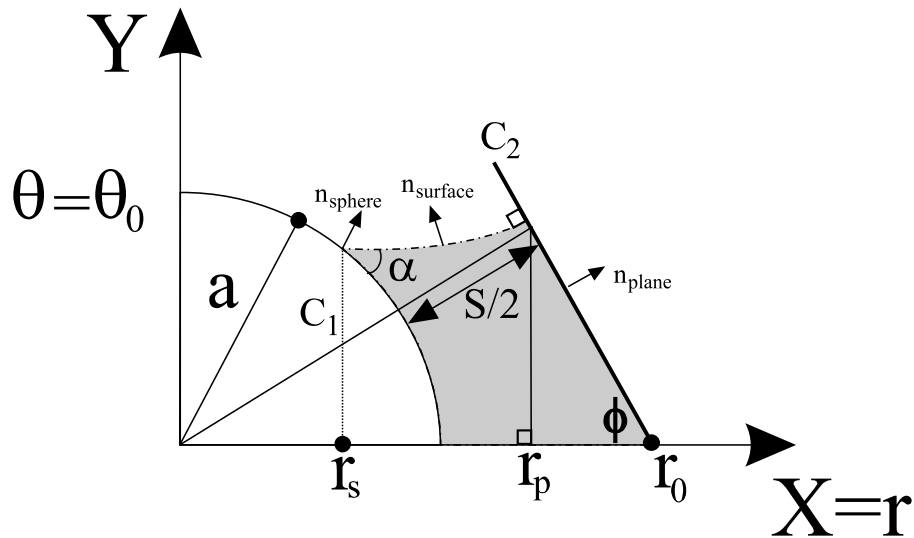
Figure 55: Variables in the region where the fluid surface is solved. Along the r axis, r_s is the fluid/sphere intersection point, r_p is the intersection between the fluid and the symmetry contour (the point r_0 occurs at the end of the mesh). S is the separation distance between spheres, and the primary particles have radius a.

The contact angle α is a physical property of the fluid satisfied along contour C_1. The angle is able to be written as

$$\alpha = \mathrm{acos}\left(n_{\mathrm{surface}} \cdot n_{\mathrm{sphere}}\right), \tag{2.59}$$

where n_{surface} is the unit outward pointing fluid surface normal, and n_{sphere} is the unit normal of the sphere. In terms of z, n_{surface} is

$$n_{\mathrm{surface}} = \frac{\mathbf{Z}_r \times \mathbf{Z}_\theta}{|\mathbf{Z}_r \times \mathbf{Z}_\theta|} = \frac{1}{\sqrt{z^2 z_r^2 + z_\theta^2 + z^2}}\left(z z_r, -z_\theta \sin\theta - z\cos\theta, z_\theta \cos\theta - z\sin\theta\right). \tag{2.60}$$

The equation of a sphere of radius a is

$$z_{\mathrm{sphere}}(r,\theta) = \sqrt{a^2 - r^2} \tag{2.61}$$

which has outward pointing normal vector

$$n_{\mathrm{sphere}} = \frac{1}{a}\left(r, \sqrt{a^2 - r^2}\cos\theta, \sqrt{a^2 - r^2}\sin\theta\right). \tag{2.62}$$

Substituting equations (2.62) and (2.60) into equation (2.59) gives an expression for α as

$$\alpha = \mathrm{acos}\left(n_{\mathrm{surface}} \cdot n_{\mathrm{sphere}}\right) = \mathrm{acos}\left(\frac{z}{a\sqrt{z^2 z_r^2 + z_\theta^2 + z^2}}\left(r z_r - \sqrt{a^2 - r^2}\right)\right). \tag{2.63}$$

When the fluid surface intersects the plane, the required condition is for the normal vector of the symmetry contour n_{plane} to be orthogonal to the fluid normal n_{surface}. This enables the continuity of z along with the partial derivatives of z. In terms of θ, the angle ϕ between the r axis and symmetry contour is $\phi = \frac{\pi}{2} - \frac{\theta}{3}$. This leads to an expression for the outward pointing normal to the symmetry contour as $n_{\mathrm{plane}} = \cos\phi(-\tan\phi, 1, 0)$. The angle between the fluid surface and the symmetry contour is

$$\beta = \mathrm{acos}\left(n_{\mathrm{surface}} \cdot n_{\mathrm{plane}}\right) = \mathrm{acos}\left(\frac{-\cos\phi}{\sqrt{z^2 z_r^2 + z_\theta^2 + z^2}}\left(z z_r \tan\phi + z_\theta \sin\phi + z\cos\phi\right)\right) \equiv 90\deg. \tag{2.64}$$

The system is solved numerically in the following section using the equations (2.58), (2.59), (2.64) derived for H, α and β.

3   NUMERICAL SOLUTION

An $n \times m$ mesh $\hat{z}_{(i,j)}$ is introduced as an approximation to $z(r,\theta)$. Indices of $\hat{z}_{(i,j)}$ reference r and θ values, where r and θ values exist at $i = 0 : \frac{r_0}{n} : r_0$ and $j = 0 : \frac{\pi}{2m} : \frac{\pi}{2}$. Central differences are used to approximate the derivatives $\hat{z}_r(i,j)$, $\hat{z}_\theta(i,j)$, $\hat{z}_{rr}(i,j)$, $\hat{z}_{\theta\theta}(i,j)$, $\hat{z}_{r\theta}(i,j)$ which appear in equations (2.58), (2.59) and (2.64). When derivates are evaluated on a boundary, such as $r = r_0$, and $\theta = 0$ and $\theta = \frac{\pi}{2}$, one sided differences (of the same order as the central differences) are used.

The constant mean curvature requirement is satisfied on 'internal' mesh points, which are mesh points other than $r = 0$ and $r = r_0$. As the system must not be over specifed, these values of r seemed to be the appropriate location at which the curvature should be relaxed to enable the boundary conditions to be satisfied. Therefore, on mesh points other than $r = 0$ and $r = r_0$, it is required that

$$\hat{P}_{(i,j)} - \hat{Q}_{(i,j)} H_0 = 0, \tag{3.65}$$

where $\hat{P}_{(i,j)}$ and $\hat{Q}_{(i,j)}$ are the numerator P and denominator Q of equation (2.58) evaluated using $\hat{z}_{(i,j)}$ and its partial derivatives. As the problem is solved on an $n \times m$ mesh, the number of unknowns (in this case the height of $\hat{z}$) is nm. Enforcing the curvature as described above provides

$(n-2)m$ equations, the contact angle between the fluid and sphere (along contour C_1) provides m equations, and m boundary conditions exist along C_2 at the symmetry contour.

In general, the boundary conditions along C_1 and C_2 occur between the mesh points of $\hat{z}_{(i,j)}$ as illustrated in figure 56. In order to determine the location of the boundary conditions, interpolation is required. To detect contour C_1, the difference between the fluid surface $\hat{z}$ and the sphere z_{sphere} is considered,

$$\hat{z}_2 = \hat{z} - z_{\mathrm{sphere}}. \tag{3.66}$$

For a particular $\theta = \theta_0$, the corresponding angle on the mesh occurs at $j = j_0$ (in the direction of θ). For $\hat{z}_{2(i,j_0)} < 0$ the fluid surface is 'internal' or to the left of the sphere, while the surface is external for $\hat{z}_{2(i,j_0)} > 0$. Using mesh points on each side of where the sphere intersects the fluid, which are $\hat{z}_{2(i,j_0)}$ and $\hat{z}_{2(i+1,j_0)}$, the angle between the sphere and fluid are evaluated using equation (2.63) as $\hat{\alpha}_{(i,j_0)}$ and $\hat{\alpha}_{(i+1,j_0)}$. Linear interpolation is used to obtain the contact angle α^* (for a particular θ),

$$\alpha^*_{j_0} = t\hat{\alpha}_{(i,j_0)} + (1-t)\hat{\alpha}_{(i+1,j_0)} \text{ where } t = \frac{\hat{z}_{2(i+1,j_0)}}{\hat{z}_{2(i+1,j_0)} - \hat{z}_{2(i,j_0)}}. \tag{3.67}$$

Interpolation is also used to determine β from equation (2.64), which is equal to 90 deg when a solution has been obtained. The symmetry contour has equation

$$z_{\mathrm{plane}} = \frac{\sqrt{3}(r_0 - r)}{\cos\theta}, \tag{3.68}$$

and to detect the position of C_2, the function

$$\hat{z}_3 = \hat{z}\cos\theta - z_{\mathrm{plane}}\cos\theta = \hat{z}\cos\theta - \sqrt{3}(r_0 - r)$$

is considered. Interpolation is used to obtain β^* which is

$$\beta^*_{j_0} = t\hat{\beta}_{(i,j_0)} + (1-t)\hat{\beta}_{(i+1,j_0)} \text{ where } t = \frac{\hat{z}_{2(i+1,j_0)}}{\hat{z}_{2(i+1,j_0)} - \hat{z}_{2(i,j_0)}}.$$

Given an initial guess of the shape of the liquid bridge (a cylinder was used in this work), the solver is required to iteratively modify the mesh solution $\hat{z}_{(i,j)}$ so that the mean curvature evaluated on the internal mesh points matches H_0 to within a specified tolerance. Similarly the contact angle α^* and angle β^* must match α and $\frac{\pi}{2}$ respectively (to within the same tolerance). In this work, the tolerance used on convergence was $f(\hat{z}) \leq 1 \times 10^{-10}$, where f is the complex function, equal to zero when a solution is obtained, involving the mean curvature, fluid/sphere contact angle, and the symmetry contour. The resolution of the mesh used was 15×15.

For fixed sphere radius a, contact angle α, and separation distance between spheres S, the one-parameter family of liquid bridges with different volumes is the mean curvature H_0 (7). Therefore, by varying H_0 as a parameter, liquid bridges of different volumes are able to be obtained.

To calculate the bridge volume, numerical integration is used to calculate the volumes V_{mesh}, V_{sphere} and V_{wedge} as illustrated in figure 56. Using these volumes, the total volume of the liquid bridge is given by

$$V = 12\left(V_{\mathrm{mesh}} - V_{\mathrm{sphere}} + V_{\mathrm{wedge}}\right). \tag{3.69}$$

As integrals, these volumes are given by

$$V_{\mathrm{mesh}} = \int_0^{\frac{\pi}{2}} \int_{r_s}^{r_p} \int_0^z z \, dz \, dr \, d\theta \tag{3.70a}$$

$$V_{\mathrm{wedge}} = \int_0^{\frac{\pi}{2}} \int_{r_p}^{r_0} \int_0^z z_{\mathrm{wedge}} \, dz \, dr \, d\theta \text{ and } V_{\mathrm{sphere}} = \int_0^{\frac{\pi}{2}} \int_{r_s}^{a} \int_0^z z_{\mathrm{sphere}} \, dz \, dr \, d\theta \tag{3.70b}$$
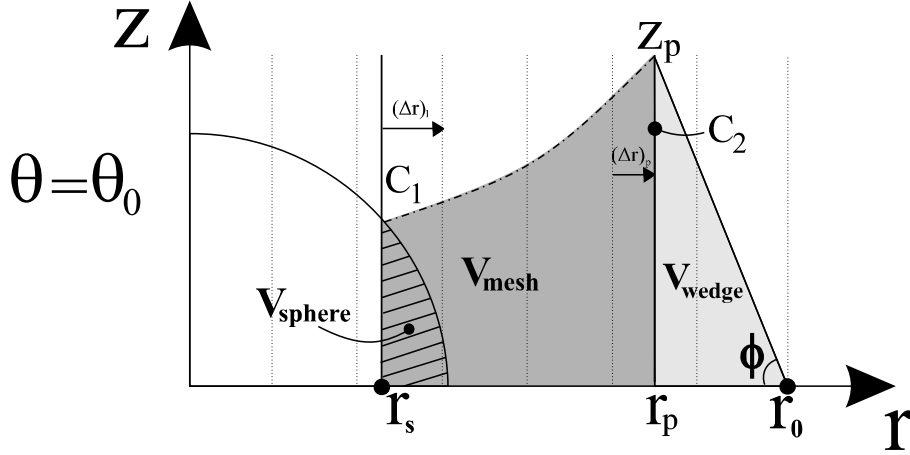
Figure 56: Computing the volume. Shaded regions are V_{sphere} (striped gray), V_{mesh} (gray) and V_{wedge} (light gray). The angle between the plane and the r axis (for given θ) is $\phi = \text{atan}\left(\frac{z_p}{r_0 - r_{\text{p}}}\right)$. The dotted vertical lines are representative of the numerical mesh in the r direction.

where z, z_{wedge} and z_{sphere} are the respective values in cylindrical coordinates of the fluid surface, the wedge portion of the bridge (the fluid surface for $r_{\text{p}} \leq r \leq r_0$), and the sphere. For each θ, the point r_p on the r axis corresponding to the intersection between the fluid surface and the symmetry contour, along with the fluid height z_{p} are able to be obtained by interpolation. Using these, the height of the wedge portion z_{wedge} at r is

$$z_{\text{wedge}} = \frac{z_{\text{p}}(r_0 - r)}{r_0 - r_{\text{p}}}. \tag{3.71}$$

Substituting equation (3.71) into the equation for V_{wedge}, and substituting equation (2.61) into V_{sphere} and integrating gives

$$V_{\text{wedge}} = \int_0^{\frac{\pi}{2}} \frac{1}{6} z_{\text{p}}^2 (r_0 - r_{\text{p}}) \, d\theta, \quad V_{\text{sphere}} = \int_0^{\frac{\pi}{2}} \left(\frac{a^3}{3} - \frac{a^2 r_s}{2} + \frac{r_s^3}{6}\right) d\theta \tag{3.72}$$

Since the values of r_s, r_p and z_p change with respect to θ, the trapezium rule is used to numerically integrate the expressions for these volumes, and obtain the volume V of equation (3.69).

The surface area of the liquid bridge is given by

$$S = 12 \int_0^{\frac{\pi}{2}} \int_{r_s}^{r_p} dS = 12 \int_0^{\frac{\pi}{2}} \int_{r_s}^{r_p} |\mathbf{Z}_r \times \mathbf{Z}_\theta| \, dr \, d\theta = 12 \int_0^{\frac{\pi}{2}} \int_{r_s}^{r_p} \sqrt{z^2(1 + z_r^2) + z_\theta^2} \, dr \, d\theta. \tag{3.73}$$

To evalutate (3.73) the function $u = \sqrt{\hat{z}^2(1 + \hat{z}_r^2) + \hat{z}_\theta^2}$ is introduced, and the surface area is evaluated numerically using the trapezium rule.

The inter-particle force between the particles is resolved at the three phase contact line (as in the approach of De Bischop and Rigole (1)),

$$F = 4\left[\gamma \int_0^{\frac{\pi}{2}} z(r_s, \theta) \sin(\delta + \alpha) \, d\theta + \Delta P \int_0^{\frac{\pi}{2}} \int_0^z z \, dz \, d\theta\right] \tag{3.74}$$

where $\delta = \text{acos}\left(\frac{r}{a}\right)$ is the angle made between the r axis and the contact point between the fluid and sphere.
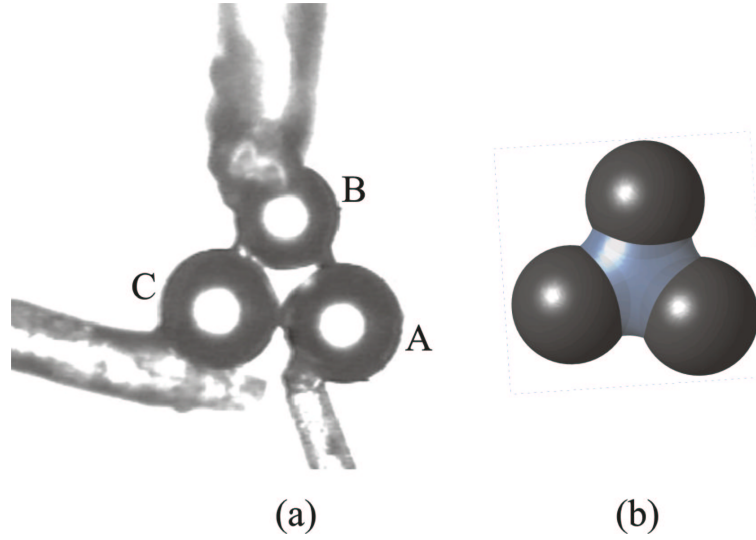
Figure 57: The experimental arrangement (a), and the result from the model (b). The volume of the figure of the left is $V = 65,596\,\mu m^3$, and the volume of the liquid bridge on the right hand side is $V = 65,923\,\mu m^3$. The two volumes agree to within 0.5 %

4 RESULTS

The methods used in this work were tested by solving for liquid bridges between two particles. This was achieved by modifying the right hand boundary C_2 from a symmetry contour to a second equally sized sphere. The results from the equation solver were compared with the solution to the ordinary differential equation (from the Young Laplace equation between two particles), and agreement was obtained with Rynhart *et. al* (2).

In the three particle case, checks regarding the scaling were made. By scaling the inter-particle separation distance as $\hat{S} = \rho S$, particle radii as $\hat{R} = \rho R$, and the mean curvature as $\hat{H}_0 = \frac{H_0}{\alpha}$, it was found that $\hat{A} = \rho^2 A$ and $\hat{V} = \rho^3 V$, indicating that the formulations for the surface area and volume from equations (3.69) and (3.73) are correct.

Figure 57(a) shows the experimental arrangement which was used to support the modelling work presented in this paper. Glass ballotini were used, the radii of the particles are $R_A = 35.4\mu m$, $R_B = 40.8\mu m$, and $R_C = 40.8\mu m$. The fluid used was glycerol which has a surface tension of $\gamma = 63.1\,mNm^{-1}$. The contact angle of the fluid was measured using a tensiometer to be 50 deg. The position of the particles A and B were measured relative to particle C located at the origin to be $(47.38 - 64.61)\mu m$ and $(86.15, 10.16)\,\mu m$ repsectively. The angles between the primary particles are $\angle AOB = 120.94\,\text{deg}$, $\angle COB = 127.32\,\text{deg}$ and $\angle COA = 111.74\,\text{deg}$. The central point O of the liquid bridge was located at $(45.59, -16.25)$ and the distance from O to each of the primary particles is $48.40\,\mu m$ (2 dp). This distance was taken to be r_0 for the model. As the model requires equally sized spheres and equal separation distances between particles, the average radius of the primary particles was taken as $\bar{R} = 39\,\mu m$ for calculation, and the position of the spheres was adjusted slightly so that $\angle AOB = \angle COB = \angle COA = 120\,\text{deg}$. While doing this, the coordinates of sphere C and the central point O were fixed, along with the distance of $48.40\,\mu m$ between O and the primary particles. The coordinates of the particles following this adjustment were $A = (54.32, -63.85)$ and $B = (82.45, 15.11)$.

Figure 5(b) shows result from the model which has $\alpha = 50\,\text{deg}$, $r_0 = 48.40\mu m$ and $H_0 = 0.0072$. The volume is $V = 65,923\,\mu m^3$ (which agrees to within 0.5% to that of the experiment). The shape of the capillary liquid bridge appears similar between the experiment and the model. The model
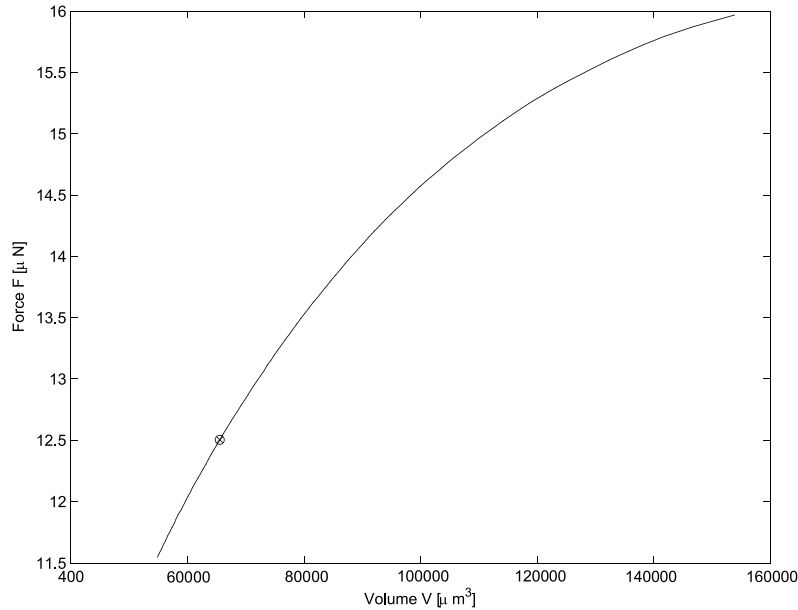
Figure 58: Relationship between the binder force between particles and liquid bridge volume for the example conditions of particle radious $\bar{R} = 39\mu m$, $\gamma = 63.1\,mNm^{-1}$. The case of figure 57 is shown as a circle on this graph. The binding force of other liquid bridges of different volumes, but with fixed α, S, $\bar{R}$, is shown above. The mean curvature was varied as a result.

was then used to calculate the inter-particle force. Figure 5 shows the relationship between the inter-particle force F and the liquid bridge volume V. The point corresponding to the experimental case is plotted having a value of $F = 12.51\,\mu N$. This is somewhat stronger than that found experimentally for two similar sized silanised glass ballotini particles, which ranges between 1 and $8\,\mu N$ depending on separation distance (8). This additional strength in a three particle agglomerate is expected because of the greater perimeter of contact at the interface boundary.

5   ACKNOWLEDGEMENTS

References

[1] De Bisschop F R E and Rigole W J L. A physical model for liquid capillary bridges between adsorptive solid spheres: The nodoid of plateau. *Journal of Colloid and Interface Science*, 88:117–128, 1982.

[2] P Rynhart, R McKibbin, R McLachlan, J R Jones. Mathematical modelling of granulation : Static and dynamic liquid bridges. *WCPT 4 conference*, page on cdrom, 2002.

[3] Urso M E D, Lawrence C J and Adams M J. Pendular, funicular, and capillary bridges: Results for two dimensions. *Journal of Colloid and Interface Science*, 220:42–56, 1999.

[4] Batchelor G K. *An Introduction to Fluid Dynamics*. Cambridge Univerisity Press, 1967. Cambridge.

[5] Dirk J. Struik. *Lectures on Classical Differential Geometry, 2nd edition.* Dover Publications Inc, 1988.

[6] D.Gilbarg, N.S. Trudinger. *Elliptic Partial Differential Equations of Second Order, 2nd edition.* Springer-Verlag, Berlin, 1983.

[7] J. M. Sullivan. The geometry of bubbles and foams. *Foams, Emulsions, and Cellular Materials, NATO Adv. Sci. Inst. Ser. C*, pages 379–402, 1998.

[8] Simons S J R and Fairbrother R J. Direct observations of liquid binder-particle interactions: the role of wetting behaviour in agglomerate growth. *Powder Technology*, 110:44–58, 2000.